

# CROSSLINKING BY PEROXIDE AND SULPHUR VULCANIZATION: CHEMICAL MECHANISMS AND REACTION KINETIC DETERMINATION

## *A Comprehensive Numerical Model*

Gabriele Milani

*Technical University of Milan, Piazza Leonardo da Vinci 32, 20133, Milan, Italy*

Federico Milani

*CHEMCO Consultant, Via J. F. Kennedy 2, 45030, Occhiobello, Rovigo, Italy*

Keywords: Vulcanization, Kinetic model, Peroxides, Accelerated sulphur, Crosslinking, Mathematical model.

Abstract: The work presents a comprehensive numerical model to optimize mechanical properties of thick rubber vulcanized items, comprising medium and high voltage electric cables and 3D devices. Several vulcanization systems are considered, including peroxides and accelerated sulphur. In the case of peroxides, both a genetic algorithm (GA) with zooming and elitist strategy and an alternating tangent (AT) approach are adopted to determine the optimal final mechanical properties (tensile strength) of 2D and 3D rubber items. The use of a mixture of peroxides is also taken into account, demonstrating that it helps in reducing the curing time and/or in increasing the optimal tensile strength in both core and skin of thick devices. For sulphur vulcanization, a mathematical kinetic model is presented to accurately predict the crosslinking density of vulcanized rubber. It bases on the actual reactions occurring in practice and allows to estimate the overall degree of vulcanization of real manufactured items.

## 1 INTRODUCTION

The matter of vulcanizing adequately thick rubber items has been in the recent past largely under-investigated, since the utilization was limited to items with thicknesses not exceeding 5 mm. The need of producing rubber insulators for medium and high voltage electric cables have made critical the problem of obtaining a sufficient vulcanization level for thick items. As a matter of fact, for thick objects, the skin results usually over-vulcanized whereas the core remains essentially under-vulcanized.

Considering that the final mechanical properties (elastic and inelastic) of the items are strongly dependent on the degree of vulcanization, it can be argued that the optimization of the vulcanization production parameters (temperature and exposition time) is critical. In particular, it has been widely shown that final vulcanized rubber mechanical properties (elastic modulus, tension set, tensile

strength, tear resistance, etc.) depend on the degree of vulcanization.

In this framework, this paper presents a comprehensive numerical model to optimize mechanical properties of thick rubber vulcanized items, comprising medium and high voltage electric cables and 3D devices. Both peroxides and accelerated sulphur vulcanization systems are considered. In the case of peroxides, both a genetic algorithm (GA) with zooming and elitist strategy and an alternating tangent (AT) approach are adopted to determine the optimal final mechanical properties (tensile strength) of 2D and 3D rubber items. The use of a mixture of peroxides is also taken into account, demonstrating that it helps in reducing the curing time and/or in increasing the optimal tensile strength in both core and skin thick items. While for peroxides the decomposition kinetic is known, and hence the reticulation level is directly dependent on the quantity of decomposed peroxide, for accelerated sulphur a comprehensive kinetic

model is still missing, Kresja & Koenig (1993). At this aim, for sulphur vulcanization, a mathematical kinetic model is presented to accurately predict the crosslinking density of vulcanized rubber. Unknown parameters of the model are numerically fitted through experimental cure curves provided by the rotor-less cure-meter RPM 2000 (ASTM D 5289) and/or rotor cure-meter (ASTM D 2084-81).

## 2 HEAT EXCHANGE MODEL: GOVERNING PARTIAL DIFFERENTIAL EQUATIONS

Temperature profiles for each point of a generic item can be obtained solving numerically a differential equation field problem representing Fourier's heat equation law, which, in its general form, may be written as:

$$\rho_p c_p^p \left( \frac{\partial T}{\partial t} \right) - \lambda_p \nabla^2 T - r_p \Delta H_r = 0 \quad (1)$$

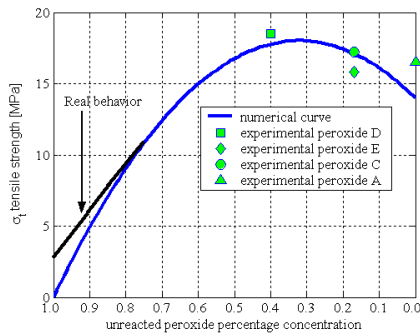


Figure 1: Non-linear behaviour of final tensile strength of an item with respect to unreacted peroxide concentration.

Where  $\lambda_p$  is the coefficient of thermal conductivity,  $c_p^p$  is the specific heat,  $\rho_p$  is rubber density,  $\Delta H_r$  is rubber specific heat (enthalpy) of reaction,  $r_p$  is the rate of cross-linking. The term  $r_p \Delta H_r$  in equation (1) is the heat required by the decomposition of the peroxide during peroxidic crosslinking.  $\Delta H_r$  usually ranges from 120 to 180 kJ/mo. From a technical point of view, the final tensile strength of a vulcanized item does not increase linearly with the curing time, but it passes from a maximum as shown in Figure 1.

Optimal  $\hat{T}$  curves (expressed as implicit functions in cure temperature  $T_c$  and  $t$ ) can be determined solving point by point the following optimization problem:

$$\max \frac{1}{N_L} \sum_{k=1}^{N_L} \sigma_t^k(T_c^i, t^i) \text{ or } \max \frac{1}{N_L} \sum_{k=1}^{N_L} F_t^k(T_c^i, t^i)$$

subject to  $\begin{cases} 0 < T_c^i < T_c^{\max} \\ 0 < t^i < t^{\max} \end{cases}$

$$\text{PDEs system} \begin{cases} \rho_j c_j^p \left( \frac{\partial T}{\partial t} \right) - \lambda_j \left( \frac{\partial^2 T}{\partial r^2} + \frac{1}{r} \frac{\partial T}{\partial r} \right) = 0 \\ \rho_p c_p^p \left( \frac{\partial T}{\partial t} \right) - \lambda_p \left( \frac{\partial^2 T}{\partial r^2} + \frac{1}{r} \frac{\partial T}{\partial r} \right) + r_p \Delta H_r = 0 \end{cases} \quad (2)$$

boundary and initial conditions

Where  $N_L$  is the number of layers in which the insulator thickness is subdivided,  $k$  is the  $k$ -th layer and  $T_c^{\max}$  ( $t^{\max}$ ) is an upper bound limitation for cure temperature (exposition time).

Two dedicated distinct models have been developed and tested by the authors to solve (2), see Milani & Milani (2008, 2009, 2010a) for algorithm details. The first one is a non-standard genetic algorithm (GA), whereas the second is an alternating tangent approach (AT), described in detail hereafter.

When an expensive grid procedure is used, for each point  $P^{i,j} \equiv (T_c^i, t^j)$  of the grid, a mixed algebraic-PDEs system is numerically solved by means of the finite element method:

$$\sigma_t = \frac{1}{N_L} \sum_{k=1}^{N_L} \sigma_t^k(T_c^i, t^j)$$

$$\rho_j c_j^p \left( \frac{\partial T}{\partial t} \right) - \lambda_j \left( \frac{\partial^2 T}{\partial r^2} + \frac{1}{r} \frac{\partial T}{\partial r} \right) = 0 \quad (3)$$

$$\rho_p c_p^p \left( \frac{\partial T}{\partial t} \right) - \lambda_p \left( \frac{\partial^2 T}{\partial r^2} + \frac{1}{r} \frac{\partial T}{\partial r} \right) + r_p \Delta H_r = 0$$

+ initial and boundary conditions

### 2.1 Peroxidic Vulcanization

For EPM/EPDM the following peroxides are ordinarily used (commercial names by Akzo): Trigonox 101 ( $t_{1/2}=0,1h$  at  $171^\circ C$ )(E), Perkadox BC ( $t_{1/2}=0,1h$  at  $162^\circ C$ )(C), Trigonox 29 ( $t_{1/2}=0,1h$  at  $138^\circ C$ )(A) and Perkadox 14 ( $t_{1/2}=0,1h$  at  $169^\circ C$ )(D). As well known, peroxides decomposition kinetic is

of first order, i.e.  $-dC/dt=kC$ . Peroxides follow the Arrhenius equation and hence the reaction constant is ruled by:

$$K(T) = K^\infty e^{-\frac{E_a}{R_g T}} \quad (4)$$

Where  $K^\infty$  and  $E_a$  are the only two constants to be determined that define completely the behaviour of the peroxide at different temperatures. Once known  $t_{1/2}$  at a given temperature, it can be easily shown that:

$$t_{1/2}(\tilde{T})/t_{1/2}(T) = e^{\frac{E_a}{R_g T} - \frac{E_a}{R_g \tilde{T}}} \quad (5)$$

Producers furnish, for each commercial peroxides, values of  $K^\infty$  and  $E_a$  or, alternatively curves of  $t_{1/2}$  at different temperatures.

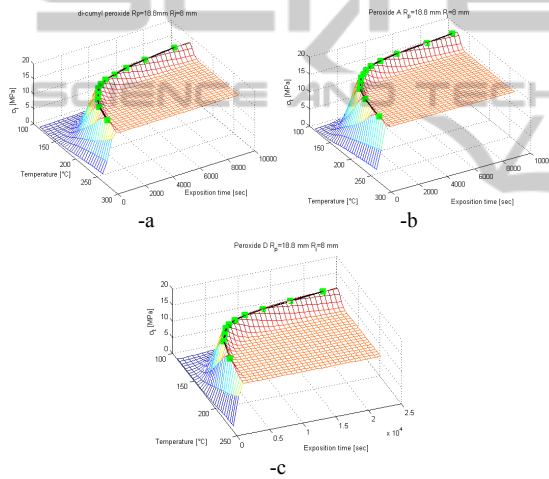


Figure 2: High voltage electric cables (green squares represent GA optimization points). Cure time-temperature-tensile strength surfaces. -a: di-cumyl-peroxide C. -b: peroxide A. -c: peroxide D.

## 2.2 GA Numerical Results

In Figure 2-a,b,c rubber mean tensile strength at different temperatures and exposition times is reported for high voltage cables, assuming as reticulation inducer three different peroxides. The 3D surface is obtained by means of the iterated solution of problem (3 on an expensive regular grid of points, whereas green squares represent the GA best fitness points. As it is possible to notice, the algorithm proposed is able to reach tensile maximum strength with sufficient accuracy for all the simulations performed.

A detailed comparison among all the results underlines that peroxide choice is crucial. Each peroxide, in fact, exhibits a different  $\hat{T}(T_c, t) = 0$  behavior; in some cases, optimal curves  $\hat{T}$  are sensibly different resulting in completely different production line parameters to select during design.

For engineering interest, we have made additional numerical simulations on realistic 3D items using again the above GA, but with mixtures of peroxides, with the aim optimizing again the curing time and the tensile strength.

When a total initial concentration  $C_0$  of two peroxides is present in the mixture, we assume that each peroxide decomposes separately, following a first order differential equation. Indicating with index 1 and 2 peroxide 1 and 2 respectively and with  $C = C_1 + C_2$  the sum of peroxides unreacted concentrations, we obtain:

$$\begin{aligned} -\frac{dC_1}{dt} &= k_1 C_1 \\ -\frac{dC_2}{dt} &= k_2 C_2 \end{aligned} \Rightarrow -\frac{d(C_1 + C_2)}{dt} = k_1 C_1 + k_2 C_2 \quad (6)$$

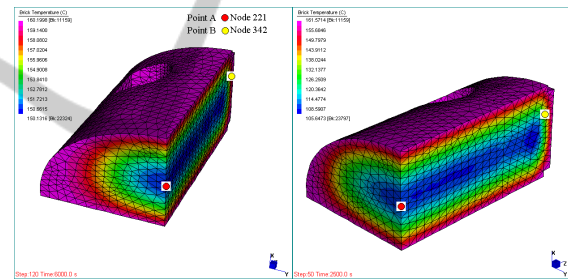


Figure 3: Temperature profile of 3D item at  $T_c = 160^\circ\text{C}$ . - a: 6000 seconds. -b: 2500 seconds.

Obviously, during vulcanization,  $T = T(t)$  and therefore a numerical integration is needed for each point of the items to vulcanize. In particular, a Finite Element FEM approach (Evans et al. 2001) is used to solve the 3D heat transmission problem. In order to have an insight into this phenomenon, in Figure 3 temperature patches for a 3D docks bumper (only  $\frac{1}{4}$  of the mesh is shown) are represented at 6000 and 2500 seconds, assuming  $T_c = 160^\circ\text{C}$  and highlighting two different nodes with colored dots (one is a node near the external surface, whereas the other belongs to the internal core). In the simulations, a 50%-50% percentage of Peroxide A and E is used.

Temperature-time, residual peroxides concentration vs time and tensile strength diagrams for the two nodes are reported in Figure 4, assuming a curing time equal to 4400 seconds. As it is possible

to notice, Point A reaches a good level of vulcanization (Figure 4-c left), which is also addressed by the residual unreacted concentration of one of the two peroxides (Figure 4-b left). On the contrary, Point B results over-vulcanized (Figure 4 right), meaning that both peroxides residual concentration is negligible. As one can note, it is particularly evident the difference in the resulting tensile strength at the end of the vulcanization process.

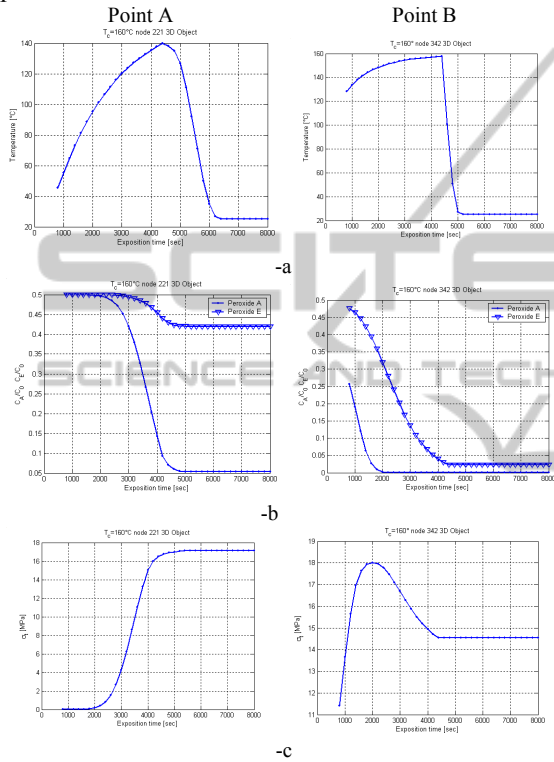


Figure 4: Point a & b response. (-a)  $t-T$ , (-b)  $t$ -peroxide concentration and (-c)  $t-\sigma_t$  curves. In the case analyzed  $\chi = 0.5$ .

### 2.3 Alternating Tangent Approach (AT)

The AT approach used in the case of the 3D item is based on the numerical evaluation of tensile strength first derivatives with respect to exposition time on several sections at fixed curing temperatures  $T_c$  and in the iterated bisection of a determined exposition time search interval.

At a fixed  $T_c$  temperature, Figure 5, tensile strength is evaluated on two starting points (points 1 and 2), usually placed at a very under-vulcanized and a very over-vulcanized exposition time. First derivatives  $d\sigma_t/dt$  of tensile strength with respect to exposition time are needed at the search interval

extremes and are determined through finite differences.

Middle point first derivative of the search interval is also needed.

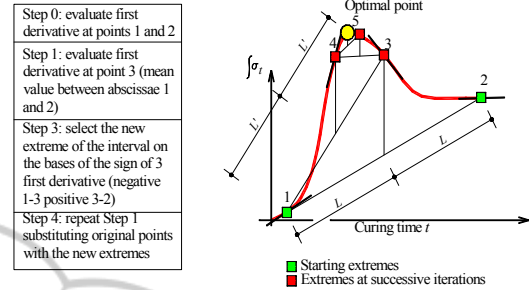


Figure 5: Alternating tangent approach (AT) basic scheme.

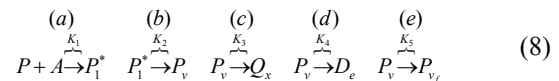
Once that first derivatives are at disposal on the search interval extremes and on the middle point, a bisection procedure is adopted, reducing the search interval to one-half. In particular, the new interval is respectively the right or the left one half depending on the sign of first derivatives of the extremes with respect to the middle point one:

$$\begin{aligned} \text{if } \left. \frac{d\sigma_t}{dt} \right|_1 \cdot \left. \frac{d\sigma_t}{dt} \right|_3 &\geq 0 \rightarrow \text{right semi - interval} \\ \text{if } \left. \frac{d\sigma_t}{dt} \right|_2 \cdot \left. \frac{d\sigma_t}{dt} \right|_3 &\geq 0 \rightarrow \text{left semi - interval} \end{aligned} \quad (7)$$

The procedure is repeated on the new reduced interval, until a desired degree of accuracy is obtained (yellow circle in Figure 5).

## 3 SULPHUR VULCANIZATION

Sulphur vulcanization chemistry is somewhat complex and has not been well understood throughout the century of the practice of the process since its discovery by Goodyear (1844). In particular, because of the prohibitive complexity of the reactions induced by sulphur during crosslinking -differently to peroxidic curing- no precise reaction kinetics formulas are available in the technical literature. However, for EPDM, the basic reactions involved are commonly accepted to be the following:



Where the symbols have the following meaning:

-  $P$  and  $A$  are the polymer (EPDM) and soluble sulphureted zinc complex(S8 + accelerators +ZnO +

stearic acid) respectively;  $P_1^*$  is the pendent sulphur (crosslink precursor);  $P_v$  is the reticulated EPDM;  $P_{v_f}$ ,  $Q_x$  and  $D_e$  are the matured cross-link, the oxidation product and diaryl-disulphide respectively,  $K_{1, \dots, 5}$  are kinetic reaction constants, which depend only on reaction temperature.

Here it is worth noting that reaction (a) in (8) represents an allylic substitution, reaction (b) is the disproportionation, whereas reactions (c) (d) and (e) occurring in parallel are respectively the oxidation, the de-sulphuration and the de-vulcanization.

From a practical point of view, it is commonly accepted that the variation of the cure-meter curve, intended as the progressive increase of rotor resistance during vulcanization, characterizes macroscopically the rubber reticulation level.

### 3.1 Kinetic Model Proposed

Chemical reactions occurring during sulphur vulcanization reported in Milani & Milani (2010b, 2011a and 2011b) obey the following rate equations:

$$\begin{aligned}
 (a) \quad & \frac{dP}{dt} = -K_1 AP \\
 (b) \quad & \frac{dP_v}{dt} = K_2 P_1^* - K_3 Q_x - K_4 D_e - K_5 P_{v_f} \\
 (c) \quad & \frac{dQ_x}{dt} = K_3 P_v \\
 (d) \quad & \frac{dD_e}{dt} = K_4 P_v \\
 (e) \quad & \frac{dP_{v_f}}{dt} = K_5 P_v
 \end{aligned} \quad (9)$$

Differentiating equation (9), after several trivial arrangements, reticulation law can be written as:

$$\frac{d^2 P_v}{dt^2} + K_2 \frac{dP_v}{dt} + \tilde{K}^2 P_v = -K_2 \frac{dP}{dt} = K_1 K_2 AP \quad (10)$$

being  $\tilde{K}^2 = K_2(K_3 + K_4 + K_5) + K_3^2 + K_4^2 + K_5^2$ .

The solution of (10) turns out to be:

$$\begin{aligned}
 P_v(t) = & C_1 e^{(\alpha+\beta)t} + C_2 e^{(\alpha-\beta)t} + \\
 & + K_1 K_2 P_0^2 \left[ (K_1 P_0)^2 - K_2 (K_1 P_0) + \tilde{K}^2 \right]^{-1} e^{-K_1 P_0 t}
 \end{aligned} \quad (11)$$

Provided that the homogeneous term is suitably substituted with an exponential function, equivalent to the original one in integral terms.

To fully solve the problem, it is necessary to determine constants  $C_1$  and  $C_2$ . They are found from initial conditions:

$$P_v(0) = 0 \quad \left. \frac{dP_v}{dt} \right|_{t=0} = K_2 P^*(0) = 0 \quad (12)$$

which lead to determine the concentration of vulcanized polymer within the mixture during the vulcanization range. The crosslinking density obeys the following closed form equation:

$$\begin{aligned}
 P_v(t) = & C_1 e^{(\alpha+\beta)t} + C_2 e^{(\alpha-\beta)t} + \rho e^{-K_1 P_0 t} \\
 C_1 = & \rho \left( \frac{K_1 P_0}{2\beta} + \frac{\alpha}{2\beta} - \frac{1}{2} \right) \quad C_2 = \rho \left( -\frac{K_1 P_0}{2\beta} - \frac{\alpha}{2\beta} - \frac{1}{2} \right) \\
 \alpha = & -\frac{K_2}{2} \quad \beta = \sqrt{(K_2/2)^2 - \tilde{K}^2}
 \end{aligned} \quad (13)$$

$$\begin{aligned}
 \rho = & K_1 K_2 P_0^2 \left[ (K_1 P_0)^2 - K_2 (K_1 P_0) + \tilde{K}^2 \right]^{-1} \\
 \tilde{K}^2 = & \tilde{K}^2 = K_2 (K_3 + K_4 + K_5) + K_3^2 + K_4^2 + K_5^2
 \end{aligned}$$

Kinetic constants to determine are only three, i.e.  $K_1$ ,  $K_2$  and  $\tilde{K}^2$ .

The most straightforward method to have a numerical estimation of kinetic constants is to fit equation (13) on experimental scorch curve, normalizing the peak value to  $P_0$  and translating the initial rotation resistance to zero, as suggested by Ding and Leonov (1996).

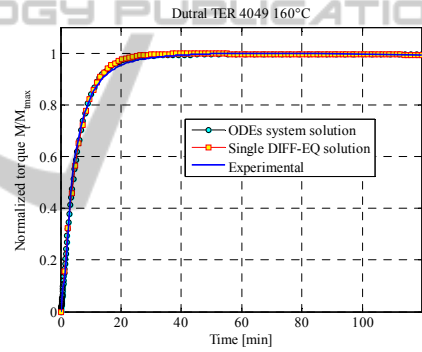


Figure 6: Dutral TER 4049 160°C. Comparison between experimental data and the numerical models proposed.

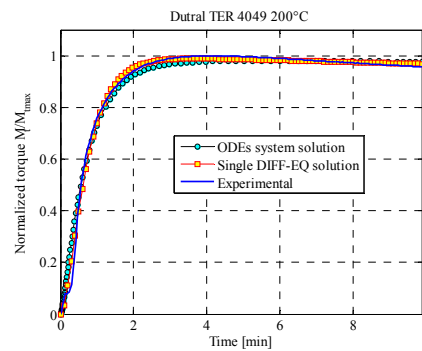


Figure 7: Dutral TER 4049 200°C. Comparison between experimental data and the numerical models proposed.

As a rule, variables  $K_1$ ,  $K_2$  and  $\tilde{K}^2$  are estimated through a standard nonlinear least square routine. Since the problem is rather easy to handle, a



trust-region-reflective algorithm is used. This algorithm is a subspace trust-region method and is based on the interior-reflective Newton method. Each iteration involves the approximate solution of a linear system using the method of preconditioned conjugate gradients (PCG).

### 3.2 Numerical Simulations

To assess model results, some experimental data available, Milani & Milani (2011b) (cure-meter curves for a commercial blend called Dutral TER 4049) are considered as reference data. To perform a numerical optimization of the kinetic model proposed, experimental cure values are normalized dividing each point of the curve by the maximum torque values, so that experimental data are always within the range 0-1. In Figure 6 and Figure 7, a comparison between cure curves provided by the present approach and experimental results is sketched for Dutral TER 4049, for a temperature equal to 160°C and 200°C. Data for 180°C are also available, but are not reported here for the sake of conciseness.

As it is possible to notice, an almost perfect agreement between the experimental data and the numerical procedure proposed is found in both cases, meaning that the simple second order differential equation model proposed may represent a valuable tool for all practitioners interested in a fast evaluation of the reticulation degree of rubber compounds vulcanized with accelerated sulphur.

## 4 CONCLUSIONS

From the results presented in this paper, the following conclusions can be drawn:

1. Both the GA and the AT approaches are able to determine optimal input parameters to optimize the production of medium and high voltage power cables, as well as of thick 3D items.
2. Numerical simulations have shown how different mixtures of peroxides may: a) reduce optimal curing time at almost constant optimized tensile strength or b) increase optimal tensile strength with an acceptable increase of curing time. Therefore, the numerical procedure proposed may represent a valuable tool for practitioners to obtain high quality vulcanized items, limiting total curing time required.
3. For sulphur vulcanization, we have proposed a mathematical kinetic model to predict EPDM compounds reticulation level, which is based on a

best fitting procedure of experimental cure curves obtained through rubber process analyzers (RPA 2000) following the ASTM D 5289 method or ASTM D 2084-81 in a predetermined temperature range. A simple second order non homogeneous differential equation model has been derived directly from the partial reactions occurring in series and parallel during vulcanization with accelerated sulphur. The model has demonstrated good performance when compared to experimental cure-curves available from a previous experimentation by the authors.

## REFERENCES

- ASTM D 2084-81 and ASTM D 5289, Standard Test Methods for Vulcanized Rubber and Thermoplastic Elastomers.
- Brydson, J. A., 1988. *Rubbery Materials and Their Compounds*, Elsevier Science Publishers LTD, Essex.
- Ding, R., Leonov, I., 1996. A kinetic model for sulfur accelerated vulcanization of a natural rubber compound. *Journal of Applied Polymer Science*, 61: 45.
- Evans, G., Blackledge, J., Yardley, P., 2001. *Numerical methods for partial differential equations*. Springer-Verlag, Berlin, 2nd edition.
- Goodyear, C., 1844. US Patent 3633.
- Kresja, M. R., Koenig, J. L., 1993. A review of sulphur cross-linking fundamentals for accelerated and unaccelerated vulcanization. *Rubber Chemistry and Technology*, 66: 376.
- Milani, G., Milani, F., 2008. Genetic algorithm for the optimization of rubber insulated high voltage power cables production lines. *Computers & Chemical Engineering*, 32: 3198-3212.
- Milani, G., Milani, F., 2009. Optimization of power cable production lines for EPM/EPDM elastomers by Genetic Algorithm with different peroxides. *Journal of Applied Polymer Science*, 111(1): 482-507.
- Milani, G., Milani, F., 2010b. Optimal vulcanization of 2D-3D EPM/EPDM thick elements through peroxidic mixtures. *Journal of Mathematical Chemistry* 47(1), pp. 229-267.
- Milani, G., Milani, F., 2010a. A new simple numerical model based on experimental scorch curve data fitting for the interpretation of sulphur vulcanization. *Journal of Mathematical Chemistry*, 48: 530-557.
- Milani, G., Milani, F., 2011a. A three function numerical model for the prediction of vulcanization-reversion of rubber during sulphur curing. *Journal of Applied Polymer Science*, 119(2), pp. 419-437.
- Milani, G., Milani, F., 2011b. Simple kinetic model fitting rheometer data for EPDM accelerated sulphur. Under review.
- Treloar, L. R. G., 1975. *The Physics of Rubber Elasticity*, 3rd ed., Clarendon Press, Oxford.